Carpathian Journal of Earth and Environmental Sciences, February 2016, Vol. 11, No. 1, p. 221 - 234

MINERALOGICAL CONSTRAINTS ON THE PETROGENESIS OF SUBVOLCANIC INTRUSIONS IN SABZEVAR OPHIOLITE (NE IRAN)

Alireza SHIRZADI[1], Seyed Jamal SHEYKHZAKARIYAYI[1], Abbas ASIABANHA REZAYI[2], Mohsen NASRABADY[2] & Chris HARRIS[3]

[1]*Islamic Azad University, Science and Research branch, Tehran, Iran.e-mail: alirezashirzadi@yahoo.com*
[1]*Islamic Azad University, Science and Research branch, Tehran, Iran.e-mail: sheikhzakariaee@srbiau.ac.ir*
[2]*Department of Geology, Faculty of Science, imam khomeyni international university, Ghazvin, Iran.e-mail: asiabanha@tmu.ac.ir*
[2]*Department of Geology, Faculty of Science, imam khomeyni international university, Ghazvin, Iran.e-mail: nasrabadi@tmu.ac.ir*
[3]*Department of Geological Sciences, University of Cape Town, Rondebosch 7701, South Africa.e-mail: chris.harris@uct.ac.za*

Abstract. The Upper Cretaceous Sabzevar Ophiolite, with an approximate area of 2000km^2, is located as a 200 km-long EW band, in the NE of Iran. According to previous work, three magmatic non-ophiolitic series are distinguished inspatial relation to this ophiolite of which the Oligo-Pliocene ADR subvolcanic rocks have been restudied in the current work with the aid of new petrographical and geochemical data. The studied rocks are distributed, as small or large dikes or domiform and coniform outcrops from the east to the west of the ophiolite. The magmatic series cover a rather extensive silica range from basaltic andesite to rhyolite (53-74 wt.%). The whole rock major element compositions define a medium K calc-alkaline subductionsuite. The rocks represent evolved melts from primitive parent. Garnet crystals in rhyolite yielded $\delta^{18}O$ value of +5.9‰, which is consistent with the derivation of the rocks from mantle-derived parental magmas with a probable restricted source contamination from subducted materials and/or slight contamination with the crust. Amphibole-plagioclase pair geothermobarometric determination indicated magmatic temperatures and pressure of mineral equilibration in the range of 549-1073°C and 2.8-10.2 kb respectively. The main mechanism of differentiation was likely fractional crystallization**.**

Keywords: amphibole, garnet, isotope, thermobarometry, sabzevar, ophiolite, subvolcanic, mantle

1. INTRODUCTION

From a global tectonic point of view, Iran is part of the Alpine–Himalayan orogenic belt that extends from the Atlantic Ocean to the Western Pacific (Bagheri & Stampfli, 2007). Most geologists believe that this belt represents the "Great Tethys Sea" once located between two large continents, Gondwana and Laurasia, during the Paleozoic–Mesozoic eras (e.g. Ghorbani, 2013; Handy et al., 2010; Sharkov et al., 2015). Being a part of such a complex geologic history, Iran is now a country made up of a mosaic of continental blocks, separated mostly by strings of Paleozoic and Mesozoic ophiolites.

Three belts of ophiolites, the remains of Paleo- and Neo-Tethys oceans have been recognized in Iran according to Lensch & Davoudzadeh (1982): A) an EW Paleozoic belt (Paleotethys oceanic crusts) restricted to the north of Iran and B) two Mesozoic belts (Neotethys oceanic crusts), one trending NW-SE, called zagros-oman-baluchestan belt; and the other bordering Central-East Iran Microplate (Upper Cretaceous).

Sabzevar ophiolite (SO), the location of the current study, belongs to the last group which, along with a few other (co-genetic?) ophiolites, is situated in "Sabzevar Zone" (Pilger, 1971) (Fig.1).

This ophiolite is investigated by earlier workers (Sadredini, 1974; Vaziritabar, 1976; Alavi-Tehrani, 1976; Lensch et al., 1977; Lensch et al.,

1979; Noghreyan, 1982; Spies et al., 1983; Baroz et al., 1983; Shirzadi, 1998; Shojaat et al., 2003; Rossetti et al., 2014; Jamshidi et al., 2015) in different aspects, but the origin of the studied suite is still debated.

The igneous post-ophiolitic rocks are scattered inside, outside or in contact with ophiolitic rocks. Spies et al., (1983) divided them into three main groups as A- Eocene andesitic-basaltic group, B- Oligocene-Pliocene andesitic-dacitic-rhyolitic domiform intrusions (the subject of present study) and C- Miocene-Pliocene alkaline rocks (alkaline basalts and shoshonitic and maintained that although the three groups are different in petrogenetic detail, they show typical island arc volcanic characters and their origin is link to the tectonic emplacement of the ophiolite and the development of a northward subduction. In the present paper, we provide new data on petrography and the chemical compositions of minerals (amphibole, feldspar, garnet) which helps further constrain the petrogenesis of the suite.

2. GEOGRAPHIC LOCATION

Sabzevar ophiolite, with an approximate length of 200 km and 3 to 22 km minimum and maximum widths, lies, as a nearly EW mountain range, in the north of Sabzevar city which itself is located in the NE of Iran (Fig. 1).

This ophiolite covers an area of about 2000km^2 as an isolated mountain range with The maximum height of 2977m at one of the subvolcanic intrusions named as "Gar mount" ("Kooh-e Gar" in Persian) located in the west of the range (Fig. l).

3. REGIONAL GEOLOGY

Referring to Baroz et al., (1983), Paleomagnetic data indicate that northern Iran had been situated at the northern rim of Gondwanaland during Devonian and Carboniferous (Wensink & Varekamp, 1980). This region probably rifted away by the end of Permian and collided with "Turan plate" in the north, in the middle Triassic (Besse et al., 1998). The Paleozoic ophiolites, mainly in the north of Iran, may testify to this collision zone. Regardless of the details, the preceding statements are in good agreement with subsequent findings of Bagheri & Stampfli (2008) and Muttoni et al., (2009). The Paleo-Tethyan suture is believed to lie north of the Alborz mountain range (Stöcklin, 1974; Berberian & King, 1981; Berberian, 1983).

Concerning the generation of oceanic crust and development of ophiolites around Central-East Iran Microplate, it could be proposed that the anticlockwise rotation of the "Lut block" (Davoudzadeh et al., 1981) might have first induced the shearing and thinning of the crust at the margins of the microcontinent along wrench faults. These steep faults might have favoured the development of short basins some of them bearing ophiolites (Baroz et al., 1983). These hypothesizes are in agreement with paleogeographic reconstructions which imply the creation of cretaceous rifts in Iran and Afghanistan during the approach of Africa to Eurasia especially during the drift of India (Stampfli, 1978).

After Paleocene, SO has suffered E-W folding. As a result of this folding, Lutetian (Middle Eocene) flysch type sediments rest, with an angular unconformity, on the subaquatic volcanosedimentary sequences of the ophiolite. In Lutetian magmatism characteristic of mature island arc commenced (Lensch et al., 1977). Basalt, andesite, dacite, alkali basalt and shoshonite erupted on the ophiolites during Eeocene, Oligo-Miocene and Miocene respectively (Lensch et al., 1980). The magmatism studied in the present work is actually the Oligo-Miocene portion of this arc magmatism.

The ages of the various subvolcanic intrusions were determined by whole-rock K-Ar method (41 to 3Ma, Spies et al., 1983) which revealed an apparent systematic age progression from south to the north in the area.

4. FIELD OBSERVATIONS AND RELATIONS

The subvolcanic intrusions are distributed both inside and outside (to the North) the ophiolite. They vary in size from small to large and are widespread throughout the entire ophiolite range. In the current study, the intrusions located inside the ophiolite are sampled and studied.

The intrusions intrude all the older ophiolitic and non-ophiolitic rock units. They are usually found as dikes, coniform and domiform bodies (Fig. 2). They are usually white, grey, light green and pink in color and the porphyritic texture can generally be observed in hand specimens. The form of the intrusions is consistent with them being the remains of shallow, subvolcanic feeding conduits (plugs), formed by erosion (erosional domes). Metamorphic effects are not usually observed around the intrusions.

In some localities amphibole-dominated clots/nodules can be seen scattered throughout the outcrops; no other significant xenoliths or enclaves were observed in the outcrops.

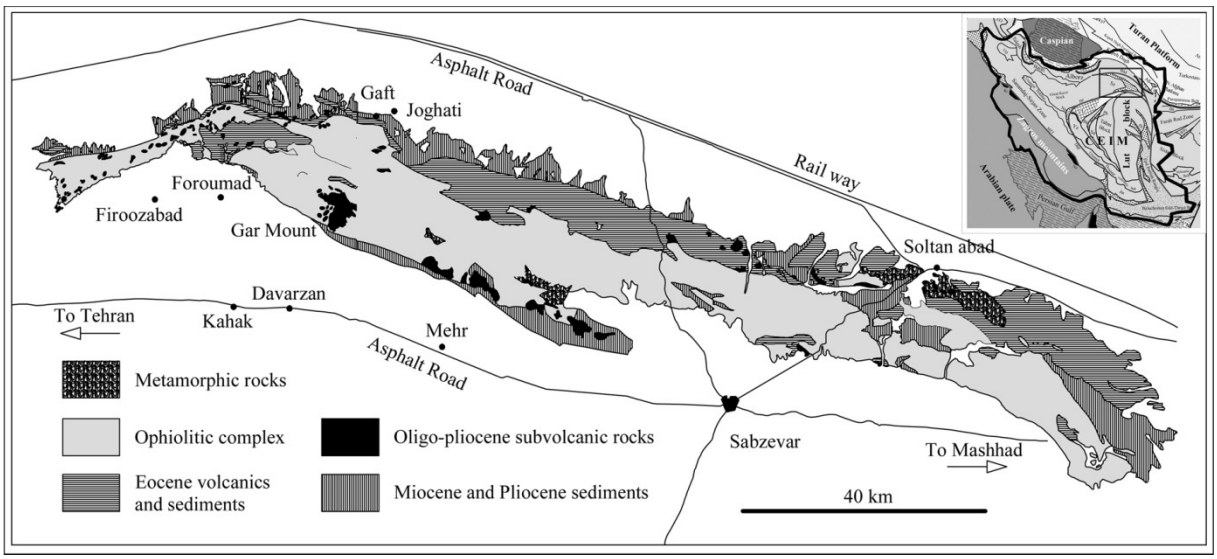

Figure 1.Geologic map of Sabzevar ophiolite (SO) simplified after "Sabzevar" and "Jajarm" 1:250,000 quadrangle map series of the Geological Survey of Iran. The studied subvolcanic intrusions can be seen scattered throughout the map (black).The rectangle in the inset marks the location of Sabzevar and the nearby ophiolites in Sabzevar Zone, Iran.

Figure 2. Field view of the subvolcanic intrusions. A medium-sized intrusion known as "Seybar" mount, located in the north of "Saroq" village. Base of the cone is about 1.4 km.

5. PETROGRAPHY

Petrographically, the studied rocks are porphyritic volcanic rocks. Petrographic work was conducted on the thin sections resulting in the following distinctions.

5.1. Rock types

Basaltic andesite and andesites, as the most primitive rock type, are strongly porphyritic and contain plagioclase, pyroxene and hornblende phenocrysts (1 to 3mm) almost in equal proportions. The phenocrysts are enclosed within a microlitic groundmass of plagioclase, clinopyroxene, magnetite (0.1 to 0.2mm) and (devitrified) glass (chlorite).

Dacites have porphyritic texture and contain mainly plagioclase, and hornblende (±quartz) phenocrysts. The phenocrysts are enclosed within a microlitic or felsitic groundmass of quartz, feldspar, biotite, magnetite and (devitrified) minor glass.

Rhyolites are usually porphyritic and consist of plagioclase, K-feldspar and quartz phenocrysts; microphenocrysts of biotite or amphibole may exist, but coexisting biotite and amphibole are rare. The phenocrysts/microphenocrysts are enclosed within a fine-grained microcrystalline quartz+ feldspar± opaques (±devitrified) glass; biotite and secondary white mica may exist.

Based on the previous works (Alavi-Tehrani, 1976; Lensch et al., 1980; Spies et al., 1983; Jamshidi et al., 2015) the rocks follow a typical calc-alkaline differentiation trend which is typical of the normal-K series. The series exhibit a relatively wide range of chemical composition from 55 to 74 wt.% SiO_2 in composition. Most of the rocks are geochemically evolved with low MgO contents (<5.9 wt.% MgO) and Mg-numbers ranging from 71 to 36.This suggests that they are not in equilibrium with normal mantle (Cox, 1980). The overall Cr and Ni contents are low (<60 and <40 ppm, respectively), reflecting the evolved nature of the rocks.

5.2. Textures

The studied rocks are mainly hypocrystalline, containing both crystals and (devitrified) volcanic glass. Glass is usually devitrified into a yellow-brown mass. The observed textures are predominantly porphyritic with microlitic, pilotaxitic, trachytic, or felsitic groundmass; Aphyric varieties exist, but are

very rare. Cumulophyric (augite+ feldspar+ Fe-Ti oxides and amphibole+ rare feldspar) and glomeroporphyritic (amphibole alone) aggregates are observed in the samples. Crystallinity increases with bulk-rock SiO_2 content and the phenocryst content varies from about 20 to 45 Vol.%.

In a few samples phenocrysts show disequilibrium textures such as sieve-textured zones of partial resorption in plagioclase phenocrysts or rounded or embayed quartz forms, suggesting at least one stage of dissolution or reaction.

5.3. Minerals assemblage

5.3.1. Major minerals

Plagioclase: Plagioclase is the most abundant mineral phase throughout the suite. It occurs as phenocrysts, microphenocrysts and as groundmass microlites. Euhedral plagioclase phenocrysts and microphenocrysts range from 0.5 up to 5mm in size. The phenocrysts show usually significant chemical zoning. Oscillatory zoning is detected in a probed plagioclase phenocryst. In two of the samples plagioclase phenocrysts exhibit sieve-textured cores (dissolution) suggesting that they are probably relict crystals from an early magma mixing event. The sieve-textured cores are enclosed by mantles of non-sieve-textured plagioclase. In some samples plagioclase phenocrysts can be seen as broken or fragmented.

Alkali feldspar: In the most differentiated rocks (rhyolite), abundant subhedral-anhedral Alkali feldspar along with anhedral quartz and phyllosilicates (white mica) form the groundmass.

Pyroxene: Clinopyroxene occurs as phenocrysts and microphenocrysts and matrix microlites in the intermediate and basic compositions. It occurs as very pale green, auhedral, eight-sided crystals in basaltic andesites and andesites. Basaltic andesite contains frequent clinopyroxene phenocrysts and densely distributed clinopyroxene microlite in the groundmass. It also occurs as subhedral grains in crystals aggregates.

Amphibole: Amphibole phenocrysts occur as individual crystals, polycrystaline aggregates or matrix microlites. It is volumetrically the major ferromagnesian mineral and occurs in nearly all rock types in the series (2-20mm). Both green and brown amphiboles exist, but the green variety is the dominant one. Crystals are usually pleochroic, twinned and zoned. The phenocrysts host inclusions of accessory phases in some of the samples. Chlorite and biotite are the most abundant replacement products. In a few samples the elongate amphibole crystals are aligned by magma flow. It is frequently surrounded by a rim of breakdown products composed of opaque Fe-Ti oxides and other fine-grained secondary minerals. Unrimmed amphiboles are rare. The rims are present only where hornblende is in contact with glass, indicating the role of the melt in the breakdown reaction. Amphibole rims are either reaction rims or black rims. Amphibole reaction rims form as pH_2O decreases during slow magma decompression (Rutherford & Hill, 1993). Black rims form on amphibole reacting with devolatilized melt at near-surface pressures (Rutherford & Devine, 2008; Thornber et al., 2008). Macroscopic two-phase amphibole+ rare feldspar clots with diameters up to 2cm are observed in one outcrop. The aggregates are composed of fine-grained green amphiboles crystals (0.1-0.5mm) and rare interstitial feldspar.

Biotite: Biotite occurs as phenocrysts and microphenocrysts and matrix microlites in acidic members of the suite. In general it is present in smaller amounts relative to amphibole. Orange to brown pleochroic phenocrysts or microphenocrysts is the dominant variety. Two textural types of biotite are present in the studied rocks: A) euhedral, solitary biotite crystals and B) anhedral biotite intergrown with hornblende. In the first case, it occurs with feldspars and quartz in the most differentiated rocks. In the latter case, it partially replaces amphibole. Inclusions of accessory phases are very common in biotite.

White mica: White mica has two occurrences. Colorless to very pale green fine-grained pleochroic grains of anhedral white mica interstitial to quartz and feldspar is predominant in the groundmass of some fine-grained highly differentiated samples. In the second case it partly replaces plagioclase as fine-grained random or oriented flakes resulted from saussuritization.

Quartz: In some silica-rich samples, quartz occurs as auhedral phenocryst or microphenocryst which shows polygonal outlines (0.5 to 3mm). In the other samples well rounded (resorbed) or embayed quartz phenocrysts are found. It also exists as anhedral small interlocking crystals in microcrystalline groundmass of acid rocks. In some samples secondary quartz occurs as a result of reaction products.

5.3.2. Accessory minerals

A variety of magmatic accessory phases are observed in thin-section from the series. Our petrographic re-examination of the rocks revealed two minerals, not reported by the previous authors: Garnet and Allanite. Apatite, zircon, titanite, allanite and Fe-Ti oxides are found as inclusions in, or as grains attached to the surface of phenocrysts or as microlites in the matrix.

Magnetite: Magnetite is an ubiquitous phase and occurs in (0.5–2 vol.%) the least to the most

differentiated rock types. It occurs as fine euhedral, subhedral or anhedral disseminations, evenly distributed throughout the groundmass. It also occurs as small crystals in the breakdown rims around the amphibole phenocrysts and as inclusion in silicate phenocrysts. Small phenocrysts and microphenocrysts are less common.

Garnet: Magmatic garnet (spessartine), as an uncommon mineral (<1 modal %), has been identified in just two of the felsic samples. The crystals are small, inclusion-free, subhedral to anhedral with an average size of 0.15 to 0.25mm. It displays no birefringence and is pale pink in plane polarized light. It is disseminated throughout the rock and coexists with biotite, quartz, K-feldspar and white mica in fine-grained rhyolites.

Apatite: Apatite is the most common accessory mineral in the suite. It is a common inclusion in phenocrysts and in the matrix in many of the samples. The crystals are euhedral (0.1-0.5 mm), display low birefringence (first order gray) and are pale pink in plane polarized light. Apatite microphenocrysts were observed in a few samples in trace amounts (<1modal %). It usually hosts unidentified mineral micro-inclusions.

Allanite: Allanite is the second widespread accessory mineral (0.05-0.15mm). The crystals are small, euhedral to subhedral, display low birefringence (first order gray) and are yellowish brown-brown in plane polarized light.

Zircon: Zircon is less common than apatite. It occurs as very small prismatic euhedral crystals (0.15-0.15 mm), display high birefringence and is pale pink in plane polarized light.

Titanite: Titanite is anhedral (up to 0.5 mm), interstitial and rare. Secondary titanite, formed by partial breakdown of ferromagnesian, is present in some samples.

6. ANALYTICAL METHODS

6.1. Major elements

Feldspar, amphibole and garnet analyses were produced with a JEOL JXA-8100 electron microprobe apparatus at the University of Cape Town (Table 1). The accelerating voltage was 15 kV, beam current 20 nA and beam size 3 microns. A mix of natural and synthetic standards for internal calibration was used.

6.2. Oxygen isotopes

A five kg sample was taken and crushed in lab from one locality and crystal separates were handpicked after standard crushing and conventional heavy-liquid density-separation techniques. Crystal separates were used for oxygen isotope determinations. Garnet crystals were pink in color, around 150-250μ in diameter and subhedral to anhedral in shape. All O-isotope ratios were measured off-line on O_2 gas, using a Finnegan DeltaXP mass spectrometer, in dual inlet mode, after extraction of oxygen by laser fluorination method at the University of Cape Town (UCT). The crystals were analyzed in duplicate. There were many grains in each analysis (each about 4.3 mg). The garnets had been cleaned in hot 10% HF before analysis to remove feldspar, quartz and other minerals. The material was probably > 95% pure garnet. The $\delta^{18}O$ values were 5.87 and 5.93 per mil. This is a good duplication – typically the precision is about +/- 0.13 (2 sigma) in that laboratory. The data are expressed on the SMOW scale as is standard. A garnet standard was used to calibrate the raw data to the SMOW scale. Details of the method are given in Harris & Vogeli (2010).

7. MINERAL CHEMISTRY

Chemical zonation in minerals reflects changes in composition, temperature, pressure and volatile content of magma (Tsuchiyama, 1985; Smith & Brown, 1988; Johannes et al., 1994). Mineral chemistry study including compositional zoning profiles on amphibole, feldspars and garnet are performed in this section. The crystals are found as phenocrysts and micro-phenocrysts as well as in the groundmass. Zoning of the phenocrysts are well evident under petrographic observation. The chemistry of minerals is investigated by using electron microprobe quantitative analyses. The crystals for chemical profiles were chosen among larger and clearly zoned phenocrysts.

7.1. Mineral chemistry and classification

Here we present new data and classification on the chemical composition of amphibole, feldspars and garnet in terms of major elements.

Amphibole: Amphibole phenocrysts are clearly zoned and euhedral up to 10 mm in length. Core and rim microprobe analyses of 15 hornblendes are presented in table 1. Formula calculation of the amphiboles and adjusting of the ferric/ferrous ratio was done according the procedure outlined in Hawthorne et al., (2012). The amphiboles names, based on Si-Ca & Li=15, are given in figure 3. The studied amphiboles are considered as members of the calcium type in which $^{B}(Ca+\Sigma M^{2+})/\Sigma B \geq 0.75$ and

$^{B}Ca/\Sigma B \geq {}^{B}\Sigma M^{2+}/\Sigma B$. $Fe^{3+}/\Sigma Fe$ ratio ranges from 0.06 to 0.67 and the average is 0.35. The studied amphiboles are named as magnesio-hastingsite, Ti-rich magnesio-hastingsite, pargasite, magnesio-hornblende and magnesio-ferri-hornblende.

Feldspar: Representative microprobe analyses are given in table 1. Figure 4 shows the composition of feldspars in the Ab-An-Or diagram. Plagioclase composition shows a great range and varies from bytownite to albite in the studied samples.

Garnet: Core and rim electron microprobe analysis results of garnets are presented in table 1. The analyses showed that the garnets are compositionally zoned almandine-spessartine solid solution. The grains exhibited relatively Mn-poorer central zones and relatively Mn-richer marginal rims. Fe^{2+}, as the second major constituent, shows an inverse correlation with Mn. The studied garnets plot in the field of magmatic garnets in Miller & Stoddard diagram (1981) (Fig. 5).

8. GARNET OXYGEN ISOTOPE

Oxygen stable isotopes ratio ($\delta^{18}O$) is a powerful tool to understand the magma origin and its evolution (e.g. Hark, 2007). Garnet has a slow rate of oxygen diffusion as described by Lackey et al., (2006). Thus the $\delta^{18}O$ value of garnet is a function of the rock in which it crystallized, the garnet/magma fractionation factor and the temperature of growth. Analysis of garnet separated from rhyolite gave $\delta^{18}O$ values of +5.87 and +5.93 ‰ which are within analytical error.

9. GEOTHERMOBAROMETRY

Two hornblende-plagioclase geo-thermometers were proposed by Holland & Blundy (1994). Thermometer A is based on the edenite-tremolite reaction (edenite + 4 quartz → tremolite + albite), which is applicable to quartz-bearing igneous rocks and thermometer B is based on the edenite-richterite reaction (edenite + albite → richterite + anorthite), which is applicable to both quartz-bearing and quartz-free igneous rocks. For this geothermometer to be applicable, plagioclase and amphibole must be co-crystallizing, equilibrium phases.

As hornblende and plagioclase commonly coexist in studied rocks, they are used for thermometric calculations. Crystallization temperatures are calculated from electron microprobe analysis of hornblende and plagioclase. The Anderson & Smith (1995) excel spread sheet is used for the calculations (Table 2). Pressures used in the temperature calculations were estimated using Schmidt's (1992) Al-in-hornblende method. Geothermometric determination Holland & Blundy (1994) indicated magmatic temperatures of mineral equilibration in the range of 549-1061°C (Table 2, Fig. 6). The crystalization pressures fall in the range between 2.8-10.2 kb.

Table 1.Amphibole, feldspar and garnet microprobe core and rim chemical analyses (wt%). am: amphibole, pl: plagioclase, gar: garnet, co: core, ri: rim. Figures in the second column are the sample numbers.

	Samp-Min	SiO_2	Al_2O_3	TiO_2	K_2O	MgO	Cr_2O_3	CaO	Na_2O	MnO	FeO	Total
1	64-am1-co	44.93	11.42	1.07	0.23	15.50	0.12	11.34	1.59	0.14	11.99	98.33
2	64-am1-hf	46.23	12.32	0.88	0.18	15.43	0.04	11.30	1.77	0.15	11.70	100.00
3	64-am1-ri1	44.28	12.61	0.90	0.20	12.63	0.07	11.01	1.51	0.22	15.11	98.55
4	64-am1-ri2	44.44	12.22	0.96	0.20	12.60	0.02	10.89	1.64	0.20	14.94	98.12
5	64-am2-co	47.07	11.15	0.77	0.18	14.89	0.09	11.16	1.56	0.15	10.88	97.91
6	64-am2-ri	46.81	10.84	0.82	0.14	14.59	0.01	10.83	1.59	0.16	12.17	97.97
7	64-am3-co	47.43	11.25	0.80	0.14	15.85	0.15	11.26	1.56	0.15	10.14	98.73
8	64-am3-hf	46.07	11.55	0.89	0.13	15.54	0.02	11.19	1.66	0.17	12.03	99.24
9	64-am3-ri	44.50	12.99	0.96	0.17	13.58	0.02	10.68	1.64	0.21	14.35	99.09
10	11-am1-co	42.23	14.66	1.55	0.35	13.51	0.02	10.84	2.21	0.25	14.18	99.81
11	11-am1-co2	41.66	14.66	1.59	0.37	13.16	0.01	10.61	2.22	0.22	14.58	99.07
12	11-am1-ri	42.25	14.30	1.54	0.35	12.79	-	10.50	2.31	0.31	14.26	98.62
13	11-am2-ajc-co	43.17	14.14	1.47	0.33	13.29	-	10.73	2.19	0.24	14.16	99.71
14	11-am2-ajc-co2	43.15	13.70	1.53	0.34	13.63	0.03	10.49	2.26	0.29	13.94	99.35
15	11-am3-co	43.30	14.00	1.45	0.32	13.44	0.02	10.55	1.96	0.29	14.47	99.80
16	28-am1-co	42.03	13.64	1.40	0.23	13.30	0.00	10.49	2.33	0.27	14.51	98.20
17	28-am1-ri	41.57	14.02	1.93	0.23	13.36	0.01	10.38	2.54	0.12	14.65	98.81
18	28-am2-co	47.44	7.22	0.85	0.14	16.99	0.05	9.68	1.64	0.31	12.54	96.86

19	28-am2-ri	42.28	12.54	1.89	0.21	13.83	0.00	10.77	2.36	0.25	13.90	98.03
20	4-am1-co	28.50	20.60	0.16	0.05	20.61	0.02	0.30	0.05	0.88	18.58	89.75
21	4-am2-co	28.47	18.92	0.03	0.04	18.35	0.01	0.33	0.11	0.82	21.06	88.14
22	18-am1-co	44.13	12.78	1.74	0.30	16.56	0.09	10.88	2.42	0.16	10.10	99.16
23	18-am1-co2	42.79	12.76	1.91	0.30	16.58	0.00	11.06	2.42	0.16	10.15	98.13
24	18-am3-co	42.77	13.70	1.26	0.48	15.29	0.02	10.63	2.56	0.14	9.46	96.31
25	18-am4-co	42.47	12.90	2.51	0.41	14.75	0.01	10.48	2.65	0.19	10.36	96.72
26	18-am5-co	40.38	16.04	1.49	0.40	12.25	-	10.60	2.35	0.21	12.68	96.40
27	64-pl2-co	56.46	28.91	0.01	0.08	0.03	0.04	10.01	5.26	0.03	0.31	101.13
28	64-pl2-co2	55.52	29.25	-	0.08	0.05	-	10.41	4.90	0.02	0.21	100.44
29	64-pl2-ri	56.97	28.20	0.01	0.10	-	-	9.40	5.53	-	0.26	100.47
30	11-pl1-co	68.56	21.55	0.00	0.06	0.02	0.07	1.41	8.97	0.05	0.02	100.71
31	11-pl1-ri	54.29	29.71	-	0.08	0.06	0.07	11.16	4.72	-	0.35	100.44
32	11-pl2	54.20	29.46	0.02	0.11	0.05	0.03	10.75	4.79	0.03	0.44	99.89
33	11-pl2-co	47.13	34.67	-	0.03	0.03	-	16.44	1.54	0.02	0.43	100.29
34	11-pl3-co	69.49	20.85	-	0.05	-	-	0.92	8.45	0.02	0.06	99.85
35	11-pl3-ri	59.09	26.62	0.05	0.21	0.01	-	7.60	6.33	0.03	0.26	100.19
36	4-pl1-ri	59.66	26.46	0.01	0.16	0.01	0.00	7.20	6.77	0.05	0.14	100.46
37	4-pl1-co	59.11	27.25	0.01	0.14	0.04	0.02	7.94	6.26	0.00	0.11	100.89
38	4-pl2-co	58.31	26.92	-	0.14	-	0.01	7.70	7.16	0.07	0.05	100.37
39	4-pl2-ri	62.72	20.05	0.00	0.37	-	-	5.26	8.08	0.03	0.01	96.53
40	28-pl1-co	67.06	21.11	-	0.08	-	0.03	1.33	9.99	0.01	0.02	99.63
41	28-pl1-ri	55.94	28.64	0.00	0.14	0.03	0.03	9.83	5.42	0.05	0.35	100.44
42	28-pl2-co	63.07	23.69	0.03	0.92	0.07	-	4.57	7.45	0.02	0.30	100.13
43	28-pl2-ri	56.70	27.45	0.01	0.17	0.05	-	9.00	5.54	0.04	0.40	99.36
44	18-pl1-co	68.83	21.11	0.02	0.07	-	0.03	0.75	9.56	0.00	0.04	100.40
45	18-pl1-ri	68.82	21.16	0.01	0.07	0.02	0.00	0.74	9.02	0.03	0.05	99.92
46	18-pl2-co	68.61	20.94	0.02	0.11	0.02	0.03	0.67	9.39	0.03	0.04	99.85
47	18-pl2-ri	68.22	21.14	0.03	0.08	0.07	-	0.77	9.24	0.04	0.18	99.78
48	2A-pl1-co	68.28	20.97	-	0.07	0.05	0.01	0.77	9.63	0.05	0.05	99.89
49	2A-pl1-ri	68.26	20.75	0.03	0.06	0.03	0.01	0.50	10.22	0.05	0.01	99.92
50	2A-pl2-co	67.97	21.57	0.03	0.51	0.02	-	0.49	9.92	0.12	0.04	100.66
51	2A-pl2-co2	68.27	21.13	0.01	0.07	0.00	-	0.79	9.31	0.03	0.00	99.62
52	2A-pl2-ri	68.46	20.55	-	0.06	0.01	0.01	0.32	9.80	0.01	0.01	99.24
53	64-pl1-co	58.21	27.75	0.00	0.10	0.02	-	8.13	6.18	0.00	0.14	100.54
54	64-pl1-ri	55.69	29.22	-	0.09	-	-	9.91	5.28	0.02	0.22	100.43
55	64-pl2-co	55.85	30.28	0.02	0.07	0.03	0.02	10.25	5.29	0.05	0.20	102.05
56	47-gar1-co	37.67	21.26	0.06	-	2.17	-	5.35	0.03	6.41	27.82	100.76
57	47-gar1-hf	37.70	21.67	0.08	-	2.19	-	5.69	-	6.56	26.04	99.93
58	47-gar1-ri1	35.16	21.42	0.02	-	0.53	-	0.18	0.03	25.61	13.92	96.87
59	47-gar1-ri2	37.53	21.48	0.05	-	1.98	-	5.47	0.00	7.69	26.84	101.05
60	47-gar1-ri3	34.73	22.00	0.01	-	0.51	-	0.20	0.03	25.88	13.72	97.08
61	47-gar2-co	37.84	21.54	0.08	-	2.33	0.00	5.56	0.04	6.45	26.41	100.25
62	47-gar2-hf	37.82	21.63	0.02	-	2.20	-	5.58	0.05	6.54	25.97	99.81
63	47-gar2-ri1	36.06	21.45	0.04	-	0.59	0.02	0.22	0.02	24.61	13.94	96.94
64	47-gar2-ri2	35.39	21.62	0.05	-	0.54	-	0.20	0.01	25.31	12.83	95.95
65	47-gar2-ri3	37.72	21.59	0.03	-	1.99	0.03	5.69	0.05	6.92	25.63	99.65
66	47-gar3-co	37.84	21.67	0.06	-	2.25	-	5.61	0.08	6.49	25.92	99.91
67	47-gar3-hf	37.28	21.45	0.05	-	2.08	0.00	5.53	0.12	6.40	25.96	98.87
68	47-gar3-ri1	36.15	21.99	0.04	-	0.90	0.00	1.14	0.05	19.54	17.23	97.04
69	47-gar3-ri2	37.72	21.45	0.06	-	2.06	-	5.63	0.07	6.93	25.52	99.45

The microprobe data for the amphiboles from the study area were also used to calculate temperature, using calibration based on Ti content in hornblende by Otten (1984). T< 970°C: T(°C)=1.204*(Ti/ 23O)+545, where Ti/23O is the number of Ti cations per unit formulae (23 oxygens) of the amphiboles. Temperature of formation estimates varies from 644 to 939°C in this method.

10. DISCUSSION

In the following section, we discuss the likely processes involved in the generation of Oligo-Pliocene subvolcanic intrusions in the SO range.

10.1. Geochemical affinities and tectonic setting

The studied volcanic-subvolcanic suite comprises mostly calc-alkaline basaltic andesites, andesites, dacites and rhyolites. From the previous works (Alavi-Tehrani, 1976; Lensch et al., 1980; Spies et al., 1983, Baumann et al., 1984), it is certain that the geochemistry of the suite corresponds to calc-alkaline magmatism of subduction-related nature.

10.2. Magma composition

The presence of hornblende can yield information on the minimum water concentration in melts with which it is in equilibrium. Below a certain fugacity of water (for a given bulk magma composition and at a given T and P), hornblende will decompose. The experiments on andesitic and dacitic compositions (Rutherford & Hill, 1993; Scaillet & Evans, 1999) indicate that at least 4 wt.% water is necessary to stabilize hornblende. This testifies to relatively high water content of the magma. The relatively high abundance of hornblende in these rocks could indicate the contribution of water from the subducting slab.

The most likely way to reconcile amphibole breakdown is to reduce the water content by reduction of pressure. The observed widespread occurrence of magnetite in the studied rocks testifies also to the development of the melts under high pO_2.

10.3. Magma evolution: textural and geochemical evidences

Magmas erupted in arc regions are generally the products of a combination of processes that occur in magma storage zones and during ascent to the surface. The compositional variability of many arc magmas is clearly controlled by storage zone processes, such as mixing, assimilation, and crystal accumulation (e.g., Hammer et al., 2002; Pichavant et al., 2002; Rutherford & Devine, 2003).

It is generally argued that evolved rock types such as andesites or dacites can be generated from more primitive basaltic precursors by complex crystal fractionation processes (e.g. Foden, 1983; Ewart & Hawkesworth, 1987; Woodhead, 1988). In continental settings it is highly likely that these involve assimilation of crustal materials and/or mixing of crustally derived melts with mantle-derived melts (e.g. McBirney, 1977; DePaolo, 1981; Grove et al., 1982; Graham & Hackett, 1987).

In the studied suite, a few samples contain plagioclase phenocrysts which exhibit sieve-textured cores suggesting they are relict crystals from an early magma mixing event. This sieve texture may be caused by resorption of the plagioclase suddenly out of equilibrium with the surrounding melt prior to growth of a different composition. (e.g. Tsuchiyama, 1985). These features suggest that the magmas were perhaps stored in an episodically replenished magma chamber during a period of time.

Dissolution of quartz alone can result from magma depressurization as quartz stability field contracts relative to feldspar in Qz-Ab-Or ternary phase diagram with decreasing pressure (Tuttle & Bowen, 1958). Resorption of quartz crystals is also reported to be the diagnostic feature of decompression crystallization (Blundy & Cashman, 2001). Based on these statements the resorption rims (corrosion gulfs), seen on quartz phenocrysts were probably mainly generated during decompression of the felsic magmas and ascent to the surface. In addition, given the quartz stability in a low temperature magma, thermal erosion and melt or fluid interaction could have also contributed to the occurrence of resorbed quartz.

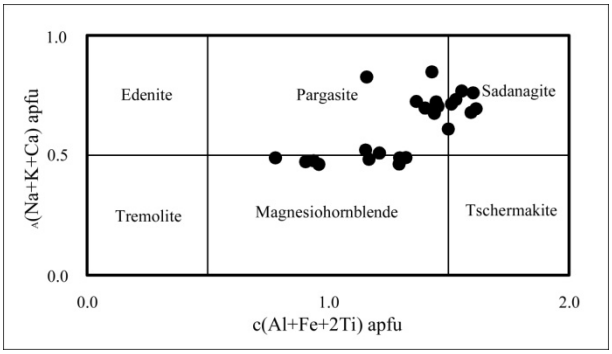

Figure 3. Calcium amphibole phenocrysts plotted on the classification diagram of Hawthorne et al., (2012). The compositions of 22 amphiboles from the studied samples are shown. Edenite, Tremolite, Sadanagaite and Tschermakite are root names. The studied amphiboles are named as magnesio-hastingsite, Ti-rich magnesio-hastingsite, pargasite, magnesio-hornblende and magnesio-ferri-hornblende.

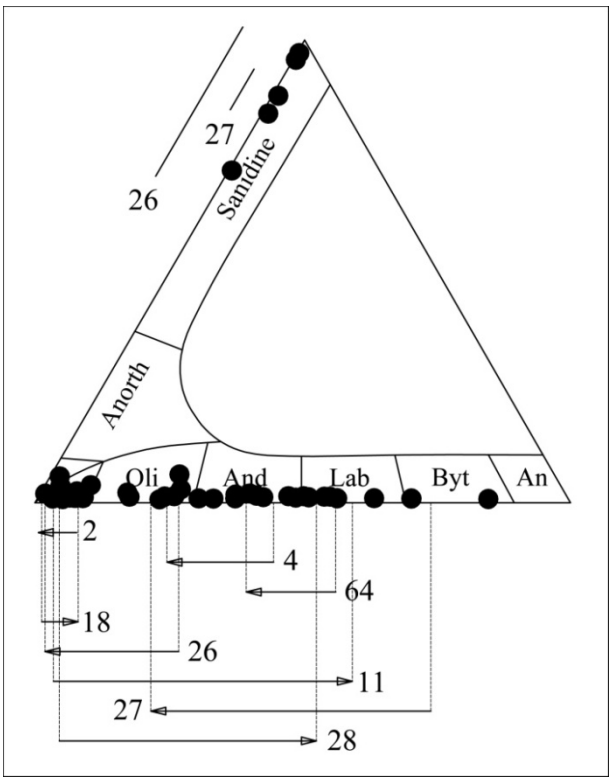

Figure 4. Composition of feldspars in the Ab-An-Or diagram. Numbers (2: trachyte, 4: andesite, 11: trachyte, 18: andesite, 26: rhyolite, 27: dacite, 28: dacite, 64: rhyolite) represent samples. Nomenclature is after Deer et al., (1966). Composition ranges are shown by bars. Flashes show core-rim compositional changes. Both normal and reverse zoning can be conceived on the diagrams.

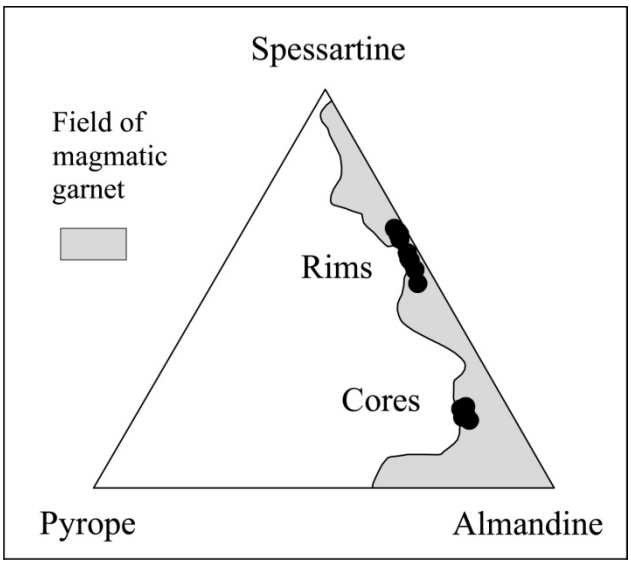

Figure 5. Ternary diagram showing compositions (Mn, Fe, and Mg) of studied garnets (open circles). The gray field is magmatic garnet compositions compiled by Miller & Stoddard (1981). Cores and rims are richer in almandine and spessartine respectively.

In a few samples quartz/feldspar phenocrysts can be seen as broken or fragmented. This may be due to fast movement of magma to the surface causing instability in crystals or by expansion and vesiculation of melt inclusions owing to depressurization during ascent.

Table 2. Maximum and minimum geothermobarometric results for subvolcanic intrusions. Temperature-pressure estimates by Holland & Blundy (1994) method, calculated from the coexisting amphibole-plagioclase pairs chemical composition. Pressures used in the temperature calculations are estimated using Schmidt's (1992) Al-in-hornblende method.

Sample	Texture	T (C) HB2 94	Pschmidt-kb
11	core	678	8.8
	core	1061	8.0
28	core	733	2.8
	rim	903	8.3
18	core	604	7.1
	core	615	10.2
64	rim	761	5.7
	rim	804	7.4
19	rim	1025	8.0
24	rim	549	8.4
	rim	899	8.4
27	rim	612	6.3
	rim	726	6.3

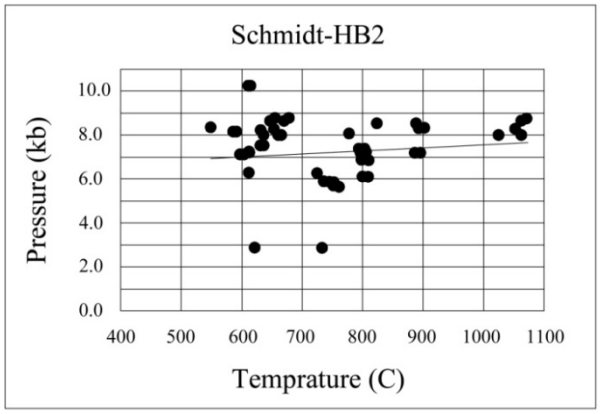

Figure 6. Pressure-temprature estimates for amphibole-plagioclas pairs cores and rims.

Chamber recharges by hotter magmas may also result in mass decrepitation of melt inclusions and crystal fragmentation in the colder magma, especially if there is an initial overheat of colder silicic magma due to delay in crystal dissolution and hence latent heat consumption (Bindeman, 1993). This provides a sufficient mechanism of >50 °C overheating, and should lead to mass decrepitation of typical melt inclusions causing crystal fragmentation. Thus corrosion and fragmentation of phenocrysts possibly indicate a dynamic magma chamber and mineral-melt disequilibria.

Rocks in equilibrium with mantle composition

have Mg numbers >70 (Wilson, 1989). This value for the studied rocks is not high enough (71-36) to be considered as primary and/or in equilibrium with mantle composition; they rather show a continuous calc-alkaline differentiation series. Some of the primitive magmas were subjected to certain processes, including fractional crystallization and magma mixing, but the main mechanism of differentiation was likely fractional crystallization, without significant contamination of the magma during its evolution. Lack of enclaves and rarity of disequilibrium minerals support crystal fractionation rather than mixing to be the principal cause of the progressive chemical changes.

10.4. Magma ascent rate and emplacement

Amphibole decompression breakdown rim can be observed in almost all the amphibole bearing samples. The rims' widths can be interpreted in terms of magma ascent rate (Rutherford & Hill, 1993; McCanta et al., 2007); the higher the ascent rates, the thinner the reaction reams. From this it can be indicated that most of the magmas rose slowly enough to cause amphibole breakdown. Unrimmed amphiboles are generally associated with explosive eruptions. The scarcity of unrimmed material in the samples is consistent with the fact that evidences of explosive activity, associated with this magmatism, are few. Apparently, ascent of magmas was slow enough for volatile exsolution leading to an effusive, not explosive, eruption in most cases.

Granophyric intergrowth of alkali-feldspar and quartz is produced as a result of undercooling of felsitic magmas (Swanson & Fenn, 1986); this texture supports the shallow-level intrusion of magma in the study area.

The predominant field and petrographic features of studied rocks indicate shallow emplacement levels as subvolcanic bodies which are inconsistent with the thermobarometric calculated depths of emplacement. By using a conversion factor of 1kb=2.6km, the crystallization depth estimate of the crystal pairs are between 7 to 27 km which is within upper to lower crustal range. The computed pressures in geothermobarometry section principally reflect the level at which the minerals crystallize rather than the pressure at which the magma consolidates; upward movement may continue after hornblende crystallization (Ghent et al., 1991).

10.5. Garnet implications

Primary igneous garnets have great petrogenetic significance because their composition depends on the magma type and the pressure and temperature under which they crystallized (Green, 1977, 1992). We used this properly to constrain the crystallization condition under which garnet was formed.

Miller & Stoddard (1981) attribute the presence of magmatic garnet in the peraluminous rocks of the Old Woman-Piute Range to late stage Mn-enrichment that took place as the granite bodies became more differentiated. Their garnets are euhedral, inclusion poor or free, up to 5mm in diameter and appeared to be in textural equilibrium with the granite. They conclude that the garnets precipitated in response to an increased ratio of Mn/Fe+Mg with differentiation. They also showed that the Mn/(Fe+Mg) ratio increases with Increasing differentiation in a melt, and argued that spessartine-rich magmatic garnet probably precipitates from evolved Mn-rich melts.

In the present study the rhyolites containing garnet represents a late residual melt, which is depleted in most of the major oxides except for K_2O, Al_2O_3 and MnO. In addition the garnets have the same features stated by the referred authors (small size, euhedral to subhedral, zoned, inclusion free and spessartine rims and almandine cores). They are formed in the most differentiated members of the series where the magma has come to the relative enrichment in Mn. The textural characteristics and chemical compositions indicate that garnet was formed by direct nucleation and subsequent crystallization from the peraluminous magma in equilibrium with solid phases such as K-feldspar.

We propose the same magmatic history for the garnets in our study. The high Mn content of the garnet implies crystallization at low temperature that prevents homogenization during growth (Spear, 1991).

10.6. Constraints from oxygen isotope: Mantle source

Garnet has a slow oxygen diffusion rate (Couglan, 1990; Vielzeuf et al., 2005) so it records the $\delta^{18}O$ of a rock at the time it crystallizes. The $\delta^{18}O$ values of the mantle and purely mantle-derived magmas are uniform at values around +5 to +6‰. Higher values indicate that magmas have been contaminated by the crust (White, 2014).

Subduction-related basalts (i.e., island arc basalts and their continental equivalents) have generally higher $\delta^{18}O$ values. This may well reflect contributions from the subducting slab. Continental subduction-related basalts are more ^{18}O rich than their oceanic equivalents, most likely due to

assimilation of continental crust (White, 2014).

The oxygen isotope fractionation between almandine garnet and magma, $\delta^{18}O$ can be estimated from the quartz-almandine fractionation of 2.0‰ at 1000°C and the quartz-magma fractionation factor of 0.6‰ of Lackey et al., (2008) for felsic magmas suggests that $\Delta^{18}O$ (garnet-magma) is -1.4‰. This means that the garnets in this study, with $\delta^{18}O$ of 5.9‰, must have crystalized from a melt with a $\delta^{18}O$ value of 7.3‰. Allowing for the increase in $\delta^{18}O$ due to fractional crystallization (0.6 ‰ e.g. Bindeman, 2008), suggest that the parent magma had a $\delta^{18}O$ value about 1.0 ‰ higher than a purely mantle-derived magma (5.7 ‰ e.g. Bindeman, 2008) and thus supports the dominantly mantle origin of the enclosing magma.

If a thick continental crust exists, crustal contamination seems inevitable (AFC) (DePaolo, 1981) and this will imparts a significant crustal isotopic signature on the rocks which is not observed in the studied samples.

It has long been understood that for evolved magmatic systems, fractional crystallization and assimilation are not decoupled processes with regard to heat balance and that the latent heat of crystallization released by fractionating phases largely contributes to the heat flux required for crustal anatexis (Goss et al., 2011).

Oxygen isotope ratios of the studied garnets are quite low ($\delta^{18}O \simeq 5.9‰$), this could suggest a mantle origin plus some input from crustal material that raised the $\delta^{18}O$ value by about 1.0 ‰. Baumann et al., (1984) determined the $^{87}Sr/^{86}Sr$ of the studied suite ranges from 0.7040 to 0.7047 which is close to mantle values. Based on the isotope and trace element results the authors exclude any considerable influence of the continental crust on the studied suite.

The studied suite appear to have a liquid lineage with mantle-derived magmas; however a differentiation path involving limited magma mixing along with crystal fractionation is involved. Subtle crustal contamination of magma is also consistent with the isotopic compositions.

11. CONCLUSIONS

The suite compositionally defines a range from basaltic (trachy)andesite, (trachy)andesite, trachyte, dacite and rhyolite. They form a continuous medium-K, calc-alkaline magmatic series. The major and trace element abundances are typical of subduction-related magmas.

The major and trace element composition of the suite is broadly in accordance with partial melting of a mantle source. The parental magmas appear to have formed above a subducting slab of dehydrating oceanic lithosphere that induced melting in the overlying mantle wedge. Crystal fractionation was the main driving process in generating the variety of daughter magmas which resulted in the formation of Si-, Al-rich differentiates. Minor magma mixing and/or shallow level assimilation may have imparted minute effects in magma features.

All available data, including field and petrographic relationships, mineral chemistry, bulk major and trace element compositions, and isotopic ratios maintain that the studied rocks are essentially co-magmatic.

The occurrence of garnet in two of the rhyolitic outcrops is due to Mn and Al enrichment in the latest stages of fractionation.

Taking into consideration the $\delta^{18}O$ values of the garnets (+5.9‰) supports the dominantly mantle origin of the lavas.

The reaction rims on many hornblende crystals probably result from decompression in the melt en route to the surface.

Abundance of amphibole and magnetite in the suite support high pH_2O and high pO_2 of magma.

Although the geochemistry of the calc-alkaline subvolcanic intrusions indicates a common origin for these rocks, their final different textures and crystallinity indicate different ascent rate and emplacement histories as a function of age and location. The intrusions were made up by magmas that are ascended from different levels and/or different parts of a deeper-seated magma chamber or chambers.

As any discernible rodingitization of the studied rocks, included in or adjacent to serpenitnized peridotites, was not observed, they must have been emplaced after serpentinization of the host peridotite and during or after ophiolite emplacement.

REFERENCES

Alavi-Tehrani, N., 1976. *Geology and petrography in the ophiolite range NE Sabzevar (Khorasan/Iran) with special regard to metamorphism and genetic relations in an ophiolite suite,* Doctorate degree thesis, university of saarbrucken, 147 p.

Anderson, J.L. & Smith D.R. 1995. *The effects of temperature and O_2 on the Al-in-hornblende barometer.* American Mineralogist, 80, 549-559.

Bagheri, S., & G. M. Stampfli, 2008. *The Anarak, Jandak and Posht-e-Badam metamorphic complex in Central Iran: New geological data, relationships and tectonic implications,* Tectonophysics, 451, 123–155,

doi:10.1016/j.tecto. 2007.11.047.

Baroz, F., Macaudiere J., Montigny R., Noghreyan M., Ohnenstetter M., & Rocci G., 1983. *Ophiolites and related formations in the central part of the Sabzevar range (Iran) and possible geotectonic reconstructions,* report 51, Geological Survey. p. 205-237.

Baumann, A., Spies, O. & Lensch, G., 1984. *Strontium Isotopic Composition of Post-OphioliticTertaryVolcanics between Kashmar, Sabzevar and Quchan/NE Iran.* Neues jahrbuch für mineralogie, geologie und paläontologie. Abhandlungen. 168, 2/3, p. 409-416.

Berberian, M., 1983. *The southern Caspian: A compressional depression floored by a trapped, modified oceanic crust,* Canadian Journal of Earth Sciences, v. 20, p. 163–183.

Berberian, M., & King, G.C.P., 1981. *Towards a paleogeography and tectonic evolution of Iran,* Canadian Journal of Earth Sciences, v. 18, p. 210–265, doi: 10.1139/e81019.

Besse, J., Torcq, F., Gallet, Y., Ricou, L. E., Krystyn, L. &Saidi, A., 1998. *Late Permian to Late Triassic palaeomagnetic data from Iran: constraints on the migration of the Iranian block through the Tethys Ocean and initial destruction of Pangaea.* Geophysical Journal International, 135, 77–92.

Bindeman, I.N., 1993. *A practical petrological method for the determination of volume proportions of magma chamber refilling.* Journal of Volcanology and Geothermal Research, 56, 133-144.

Bindeman, I.N., 2008. *Oxygen isotopes in mantle and crustal magmas as revealed by Single Crystal Analysis,* Reviews in Mineralogy and Geochemistry, Vol. 69 pp. 445-478.

Blundy, J. & Cashman, K., 2001. *Ascent-driven crystallization of dacite magmas at Mount St Helen, 1980-1986.* Contribution to mineralogy and petrology, 140: 631-650.

Couglan, R. A. N., 1990. *Studies in diffusional transport: Grain boundary transport of O in feldspars, diffusion of O, strontium, and the REEs in garnet and thermal histories of granitic intrusions in south-central Maine using O isotopes.* Ph.D. thesis, Brown University, Providence, RI.

Cox, K.G., 1980. *A model for flood basal volcanism.* Journal of Petrology, 21, p. 629-50.

Davoudzadeh, M., Soffel, H. & Schmidt, K., 1981. *On the rotation of the Central-East-Iran microplate.* Neues Jahrbuch fur Geologie und Palaontologie Abhandlungen, 3: 180-192.

Deer, W. A., Howie, R. A., & Zussman J., 1966. *An introduction to the rock-forming minerals.* London: Longman Group, pp 528.

DePaolo, D. J., 1981. *Trace elements and isotopic effects of combined wallrock assimilation and fractional crystallisation.* Earth and Planetary Science Letters 53, 189–202.

Ewart, A. & Hawkesworth, C. J., 1987. *The Pleistocene–recent Tonga–Kermadec arc lavas: interpretation of new isotopic and rare earth data in terms of a depleted source model.* Journal of Petrology 28, 495–530.

Foden, J. D. 1983. *The petrology of the calc-alkaline lavas of Rindjani Volcano, east Sunda arc: a model for island arc petrogenesis.* Journal of Petrology 24, 98–130.

Ghent, E.D., Nicholls, J., Siminy, P.S., Sevigny, H.H., Stout, M.Z., 1991. *Hornblende geobarometry of the Nelson Batholith, Southeastern British Columbia: tectonic implications.* Canadian Journal of Earth Science 28, 1982–1991.

Ghorbani, M., 2013. *The Economic Geology of Iran,* Springer, 569 pp.

Goss, A. R., Kay, S. M., Mpodozis, C., 2011. *The geochemistry of a dying continental arc: the Incapillo Caldera and Dome Complex of the southernmost Central Andean Volcanic Zone.* Contribution to Mineralogy and Petrology, 161:101–128.

Graham, I. J. & Hackett, W. R., 1987. *Petrology of calc-alkaline lavas from Ruapehu Volcano and related vents.* Journal of Petrology 28, 531–567.

Green, T.H., 1977. *Garnet in silicic liquid and its possible use as P–T indicator.* Contribution to Mineralogy and Petrology, 65, 59–67.

Green, T. H., 1992. *Experimental phase equilibrium studies of garnet-bearing I-type volcanic and high-level intrusives from Northland, New Zealand.* Transactions of the Royal Society of Edinburgh: Earth Sciences, 83, 429-438.

Grove, T. L., Gerlach, D. C. & Sando, T. W., 1982. *Origin of calcalkaline series at Medicine Lake volcano by fractionation, assimilation, and mixing.* Contributions to Mineralogy and Petrology, 80, 160–182.

Hammer, J.E., Rutherford, M.J., 2002. *An experimental study of the kinetics of decompression-induced crystallization in silicic melt.* Journal of Geophysical Research 107, ECV8-1–ECV8-24.

Handy, M. R., Schmid, S. M., Bousquet, R., Kissling, E., Bernoulli, D., 2010. *Reconciling plate-tectonic reconstructions of Alpine Tethys with the geological–geophysical record of spreading and subduction in the Alps.* Earth-Science Reviews 102, p 121–158.

Hark, Jessica S., 2007. *"Origins of Garnet in Peraluminous Granitoids Found in the South Mountain Batholith, Nova Scotia".* Senior Independent Study Theses**.** Paper 1826.

Harris, C., & Vogeli, J., 2010. *Oxygen isotope composition of garnet in the peninsula granite.* South African Journal of Geology, Vol: 113.4 Page: 401-412.

Hawthorne, F. C., Oberti, R., Harlow, G. E., Maresch, W. V., Martin, R. F., Schumacher, J. C., Welch, M. d., 2012. *Nomenclature of the amphibole supergroup.* American Mineralogist, Volume 97, p

2031–2048.

Holland, T. & Blundy, J., 1994. *Non-Ideal Interactions in Calcic Amphiboles and Their Bearing on Amphibole–Plagioclase Thermometry.* Contribution to Mineralogy and Petrology, vol. 116, no. 4, pp. 433–447.

Jamshidi, K., Ghasemi, H., Troll, V. R., Sadeghian, M., &Dahren, B., 2015. *Magma storage and plumbing of adakite-type post-ophiolite intrusions in the Sabzevarophiolitic zone, NE Iran.*Solid Earth Discuss., 6, 2321-2370, doi:10.5194/sed-6-2321-2014.

Johannes, W., Koepke, J. & Behrens, H., 1994. *Partial melting reactions of plagioclase bearing systems.* In: Parson I. (Ed.), Feldspars and Their Reactions. Kluwer, Dordrecht, pp. 161-194.

Lackey, J.S., Valley, J.W., & Hinke, H.J., 2006. *Deciphering the source and contamination history of peraluminous magmas using delta^{18}O of accessory minerals: examples from garnet-bearing plutons of the Sierra Nevada Batholith*. Contribution to Mineralogy and Petrology, v. 151, p. 20-44.

Lackey, J. S., Valley, J. W., Chen, J. H. & Stockli, D. F., 2008. *Dynamic magma systems, crustal recycling, and alteration in the central Sierra Nevada batholith: the oxygen isotope record.* Journal of Petrology, 49, 1397-1426.

Lensch, G., Mihm A., & Alavi-Tehrani, N., 1979. *Major element geochemistry of ophiolites north of Sabzevar (Iran).* Neues jahrbuch fur mineralogy, geologie und palaontologie.Abhandlungen7, 415–447.

Lensch, G., Mihm, A. & Alavi-Tehrani, N., 1977. *Petrography and Geology of the Ophiolite Belt North of Sabzevar/Khorassan (Iran).* Neues Jahrbuch fur Mineralogie - Abhandlungen. 131, 2, p. 156-178.

Lensch, G., Mihm, A. & Alavi-Tehrani, N., 1980. The postophiolitic volcanism north of Sabzevar/Iran: geology, petrography and major element geochemistry. Neues Jahrbuch für Geologie und Paläontologie–Monatshefte 686–702.

Lensch, G. & Davoudzadeh, M., 1982. *Ophiolites in Iran.* Neues Jahrbuch fur Mineralogy, geologie und palaontologie. Abhandlungen.5, p. 306-320.

McBirney, A. R., 1977. *Mixing and unmixing of magmas.* Journal of Volcanology and Geothermal Research 7, 357–371.

McCanta, M. C., Rutherford, M. J., & Hammer, J. E., 2007. *Pre-eruptive and syn-eruptive conditions in the Black Butte, California dacite: Insight into crystallization kinetics in a silicic magma system;* Journal of Volcanology and Geothermal Research 160, 263–284.

Miller, C.F., & Stoddard, E.F., 1981. *The role of manganese in the petrogenesis of magmatic garnet: an example from the Old-Woman-Piute Range, California.*Journal of Geology, 89, 233–246.

Muttoni, M., Mattei, M., Balini, M., Zanchi, A., Gaetani, M., & Berra F., 2009. *The drift history of Iran from the Ordovician to the Triassic.* In: Brunet M.F., Markus Wilmsen M. & Granath J. W. (eds.), South Caspian to Central Iran Basins. Geological Society of London Special Publications, 312, 7-29, doi: 10.1144/SP312.2.

Noghreyan, M. K., 1982. *Evolution geochimique, mineralogique et structurale d'un edifice ophiolitique singulier: le massif de Sabzevar (partie centrale), NE de l'Iran.* These Doc d'Etat, Universite de Nancy, France. pp 240.

Otten, M.N., 1984. *The origin of brown hornblende in the Artjallet gabbro.*Contribution to Mineralogy and Petrology, 86, 189-199.

Pichavant, M., Martel, C., Bourdier, J. L. & Scaillet, B., 2002. *Physical conditions, structure, and dynamics of a zoned magma chamber; MountPelee (Martinique, Lesser Antilles arc).* Journal of Geophysical Research 107, ECV 1-1.

Pilger, A., 1971. *Die zeitlich-tektonische Entwicklung der iranischen Gebirge.,* Clausthaler Geologische Abhandlunger 8, Clausthal, 8; 27 pp.

Rossetti, F., Nasrabady, M., Theye, T., Gerdes, A., Monié P., Lucci, F. & Vignaroli, G., 2014. *Adakite differentiation and emplacement in a subduction channel: The late Paleocene Sabzevar magmatism (NE Iran).* Geological Society of America Bulletin, vol. 126; no. 3/4; p. 317–343; doi:10.1130/B30913.1.

Rutherford, M. J., & Hill, P. M., 1993. *Magma ascent rates from amphibole breakdown: An experimental study applied to the 1980–1986 Mount St. Helens eruptions.*Journal of Geophysical Research, Vol 98, issue B11, pp 19667–19685.

Rutherford, M. J. & Devine, J. D., 2008. *Magmatic conditions and processes in the storage zone of the 2004-2006 Mount St. Helens Dacite.* In: Sherrod, D. R., Scott, W. E. & Stauffer, P. H. (eds) Avolcano rekindled; the renewed eruption of Mount St. Helens, 2004-2006. US Geological Survey, Professional Paper 1750, 703-726.

Rutherford, M.J., & Devine, J.D., 2003. *Magmatic conditions and magma ascent as indicated by hornblende phase equilibria and reactions in the 1995–2002 Soufriere Hills magma.* Journal of Petrology 44, 1433–1453.

Sadredini, E., 1974. *Geologie and petrographie in mittelteil de ophiolith zugesnordlechen Sabzevar (Khorasan/Iran).* Doct Theses University of Saarbrucken, 120 P.

Scaillet, B., & Evans, W. E., 1999. *The 15 June 1991 eruption of Mount Pinatubo. I. Phase equilibria and pre-eruption p-t-fO$_2$-fH$_2$O conditions of dacite magma*. Journal of Petrology, 40, 381–411.

Schmidt, M. W., 1992. *Amphibole composition in tonalite as a function of pressure: An experimental calibration of the Al-in-hornblende barometer".* Contrib Mineral Petrol, 110, p 304-310.

Sharkov, E., Lebedev, V., Chugaev, A., Zabarinskaya,

L., Rodnikov, A., Sergeeva, N., & Safonova, I., 2015. *The Caucasian-Arabian segment of the Alpine-Himalayan collisional belt: Geology, volcanism and neotectonics*, Geoscience Frontiers. Vol 6, Issue 4, P 513-522.

Shojaat, B., Hassanipak, A. A., Mobasher, K. & Ghazi, A. M., 2003. *Petrology, geochemistry and tectonics of the Sabzevarophiolite, North Central Iran.* Journal of Asian Earth Sciences 21, 1053–1067.

Smith, J.V. & Brown W.L., 1988. *Crystal structures, physical, chemical and microtextural properties*, Berlin, Heidelberg, New York, Springer Verlang, pp 828.

Spear, F.S., 1991. *On the interpretation of peak metamorphic temperatures in ligth of garnet diffussion during cooling*. Metamorphic Geology, 9, 379-388.

Spies, O., Lensch, G. & Mihm, A., 1983. *Geochemistry of the post-ophiolitic Tertiary volcanics between Sabzevar and Quchan/NE-Iran.* Geological Survey of Iran: Geodynamic Project (Geotraverse) in Iran, Final Report. Report Nr. 51, p. 247-265.

Shirzadi, A., 1998. *Petrography, petrology and geochemistry of Sabzevar Ophiolite ophiolitic and post-ophiolitic rocks, in the north of foroumad village (NE Iran).* MSc dissertation, Azad University, North Tehran Branch, Tehran, Iran. In Persian, abstract in English.

Stampfli, G.M., 1978. *Etude geologique generale de l'Elbourz oriental au sud de Gonbad-e-Qabus, Iran NE*. These Génève, 329 pp.

Stöcklin, J., 1974. *Possible ancient continental margins in Iran.* In Burke, C., & Drake, C., eds., The geology of continental margins: New York, Springer-Verlag, p. 873–887.

Swanson, S. E. & Fenn, P. M., 1986. *Quartz crystallization in igneous rocks.* American Mineralogist 71, 331–342.

Thornber, C. R., Pallister, J. S., Lowers, H. A., Rowe, M. C., Mandeville, C.W. & Meeker, G. P., 2008. *Chemistry, mineralogy, and petrology of amphibole in Mount St. Helens 2004-2006 dacite.* In: Sherrod, D. R., Scott, W. E. & Stauffer, P. H. (eds) Avolcano rekindled; the renewed eruption of Mount St. Helens, 2004-2006. US Geological Survey, Professional Paper 1750, 727-754.

Tsuchiyama, A., 1985. *Dissolution kinetics of plagioclase in the melt of the system diopside–albite–anorthite, and origin of dusty plagioclase in andesites.* Contributions to Mineralogy and Petrology 89, 1–16.

Tuttle, O. F. & Bowen, N. L., 1958. *Origin of granite in the light of experimental studies in the system* $NaAlSi_3O_8$-$KAlSi_3O_8$-SiO_2-H_2O. Geological Society of America Memoir 74, 153 pp.

Vaziritabar, F., 1976. *Geologie and petrographie der ophiolithe und ihrervulcanosedimentaren Folgeprodukteimostleil des Bergzugsnordlich Sabzevar Khorasan (Iran).* Thesis, University of Saarbrucken, 152P.

Vielzeuf D., Veschambre M., & Brunet F., 2005. *Oxygen isotope heterogeneities and diffusion profile in composite metamorphic-magmatic garnets from the Pyrenees.* American Mineralogist 90, 463–472.

Wensink, H. & Varekamp, J.C., 1980. *Paleomagnetism of basalts from Alborz: Iran part of Asia in the Cretaceous*. Tectonophysics, volume: 68, pp. 113-129.

White, W. M., 2014. *Isotope Geochemistry.* (1): pp 400. Oxford: Wiley-Blackwell.

Wilson, M., 1989. *Igneous Petrogenesis. A Global Tectonic Approach*. Unwin Hyman, 466 pp.

Woodhead, J. D., 1988. *The origin of geochemical variations in Mariana lavas: a general model for petrogenesis in intra-oceanic island arcs?* Journal of Petrology 29, 805–830.

Received at: 15. 06. 2015
Revised at: 04. 12. 2015
Accepted for publication at: 11. 12. 2015
Published online at: 18. 12. 2015